Evaluating the Pan-STARRS Variability Parameter

Daichi Hiramatsu[1, *] and Corey Mutnik[1, †]

[1]*Department of Physics & Astronomy,*
University of Hawai'i at Mānoa

By Thursday (4/18) we need: well thought out section titles and plots that show all the points we wanna make

remake prob(f) plot with all 300,000 stars (not only 80,000)

LS analysis on ATLAS Pathfinder Telescope data, verified PS variability criteria

1. INTRODUCTION

- why we care

- what made us care about this project

- NO structure / distance stuff (maybe put it in looking forward section at end)

- talk about PS catalog

- variability surveys (discuss other attempts to measure variables across the sky)

- why are variables interesting

- Summary: we ran LS, analyzed stars, why did we do it all

- Mention what will be discussed: "in section 2 we describe the observations we used..."

2. ATLAS PATHFINDER OBSERVATIONS

We used the 0.18 m Asteroid Terrestrial-impact Last Alert System (ATLAS) Pathfinder telescope[?] at the Mauna Loa. The field of view (FOV) of the telescope is $5.2°$ with the angular resolution (effective PSF FWHM) of 5". Thanks to its wide FOV, it is suitable for our project, wide field study. The spatial resolution, however, is not great. For this reason, we chose our field to be slightly off the galactic plane.

2.1. SNR Calculation

To calculate an appropriate sampling frequency and SNR, typical RR Lyrae light curves[?] were used with artificially introduced gaps and noise following the Gaussian distribution. To determine distances from the PL relations[?] within $\simeq 5\%$ accuracy assuming typical metalicity $Z = 0.001$, we need periods within $\simeq 1\%$ accuracy. The period range of RR Lyrae stars is 0.05 to 1.2 days [?] which contrains the sampling frequency. By using the Lomb-Scargle analysis (discussed in § 4), it was found that 15 nights with 10 observations/night is the lower limit sampling duration and rate to achieve the desired period accuracy. Since the magnitude fluctuations of RR Lyrae are typically in the range of 0.3 to 2.0 mags [?] , the uncertainty in magnitude was taken to be 0.1 mags, and the changes, 0.01 to 0.1 mags, in the uncertainty did not affect the period determinations significantly. Thus we only needed 10% photometry. For $m_g = m_r = 16$ and $m_i = 15.7$, an exposure time of 20 sec yields 10% photometry for the ATLAS pathfinder telescope[?] .

- we used data from ATLAS

- supplemented with ATLAS data [REF TONRY] (possibly make this s subsection)

- what was the weather like during observations

- PSF FWHM variations (only include if we discuss crowding)

- 'we recieved the reduced image data from the ATLAS pipeline; which gave us RA, Dec, mag, etc...'

- `http://fallingstar.com/how_atlas_works.php`

[VERIFY CORRECT CITATIONS:
Initially, determination of variability was going to be achieved using data collected by the *griProject*[?] . The *griProject* is [EXPLAIN]...
In order to reduce aliasing, extra observations needed to be made. Observation procedures are discussed in § 2 2.2. [PATHFINDER USED FOR GRI DATA...the reduction process is discussed at length Tonry in...cite]
We received the reduced image data from the ATLAS pipeline[?] [?]

2.2. Data Collection

[NEED TO CITE TONRY FOR OUR OBSERVATIONS]

[MENTION THAT OUR OBS NECESSARY TO REDUCE ALIASING]

Using the Pathfinder telescope, observations were made at two galactic latitudes ($b^{II} = \pm 5°$) and spanned a range of galactic longitudes ($202° < l^{II} < 232°$). Observations discussed here indicated the center of each FOV. Exposures were collected for 20 s and separated by 3° longitudinally. For implementation by the Pathfinder telescope, a conversion to RA and Dec was made; giving a range of $93 < RA < 119°$ and $-20° < Dec < 13°$, as shown by Figure 9. To account for the 0.05 ° gap between the detectors, a 0.1 ° offset in RA was implemented on every other night. Spanning 20 nights, 10 observations a night were collected on 3/8/16-3/27/16. Luckily, all of these nights had weather perfectly attuned for observations. Half a night of observations were lost on 3/19/26, due to a crash of the server controlling the telescope.

Observations were traced out by moving the FOV by 3° longitudinally, starting at $b^{II} = -5°$, $l^{II} = 202°$ and ending at $b^{II} = -5°$, $l^{II} = 232°$. Once observations at $b^{II} = -5°$ were complete, the FOV was shifted to $b^{II} = +5°$, $l^{II} = 232°$.

2.3. Object Cuts

Various data points, reduced by the ATLAS pipeline[?] , were returned with magnitude errors of zero. Such values were not used determining variability of the source. In order for an identified star to be considered for variability testing, we required a minimum of 12 "good" observations. A "good" detection is meets the minimum PSF, does not fall on the edge of each 1 deg^2 FOV, and was observed with clear skies. A minimum of 12 observations was deemed necessary, in order to eliminate aliasing, as discussed in § 4. After observation cuts were applied, 1.5 Billion stars remained in our FOV.
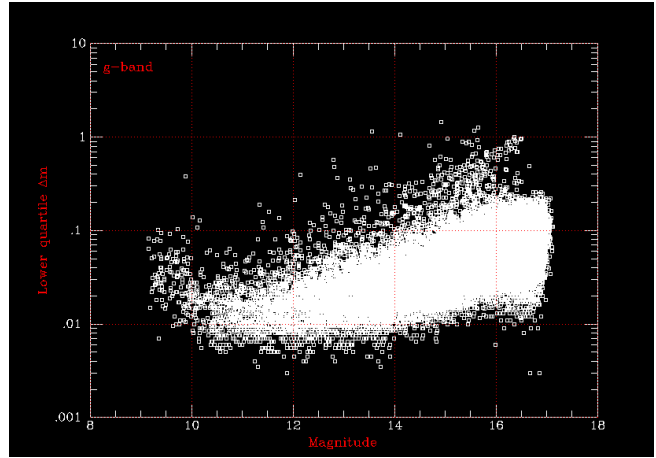

FIG. 1: *Lower quartile variance as a function of magnitude.*

In order to exploit the lower quartile variance, shown in Figure ??, a factor of $0.2m$ was added to account for Poisson error. The higher a star deviates from the average value, the more likely it is variable.

As a result of running FLS, the most variable candidates fell below $logPr(rnd) = -45$, shown in Figure 3.

[DESCRIBE logPr(rnd)...how some vars might have slipped past, but only]
[CITE WHERE IT SAYS RRLYRAE HAVE 0.5 ¡ PERIOD ¡ 1.2 [DAYS]]

3. CONSTRUCTING STELLAR LIGHT CURVES

• how we selected stars (12+ obs, 1x1 deg^2, etc)

The selection process began

4. PERIODOGRAM ANALYSIS

To extract periods from light curves, the Fast Fourier Transform (FFT) is usually used. For our data, however, FFT is not optimal due to the data gaps. To deal with the data gaps, the Fast Lomb-Scargle (FLS) periodogram analysis[?][?] was used in this study because of its high computational efficiency. FLS extracts not only periods but also the significance levels of periods in the form of $\log Pr(rnd)$. The more negative the significance levels are, the more significant the periods are, so we can used the significance levels to statistically select periodic-variable candidates. The outputs, $\log Pr(rnd)$ and frequency, of FLS is shown in FIG. 3. Since our observational period is roughly a day, there are major aliasings at the periods with integer
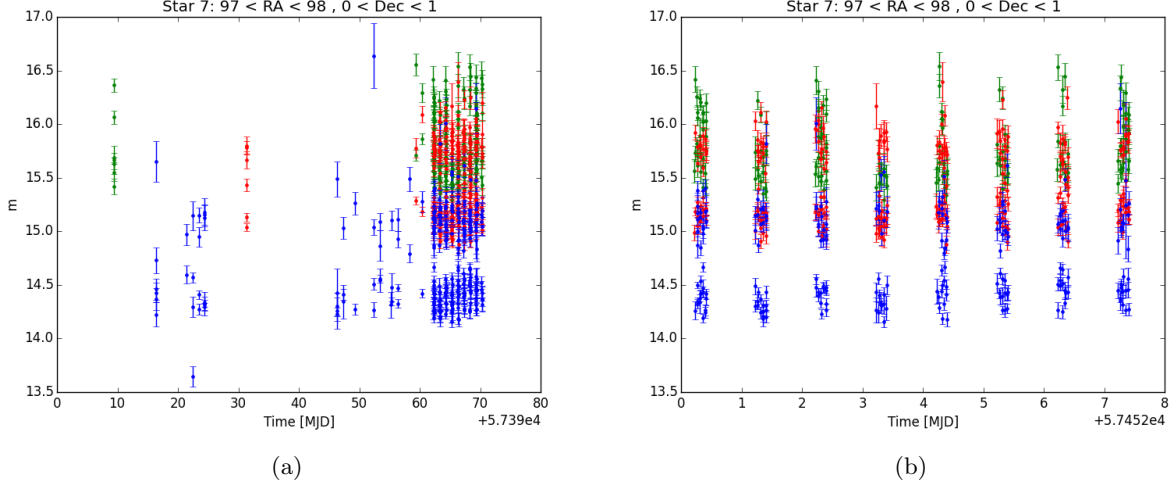
(a)

(b)

FIG. 2: *Light Curve of a variable star. Panel '(a)' shows a light curve constructed using all collected and ATLAS data. Panel '(b)' is a restricted selection of '(a)', not showing any observations made by ATLAS.*

multiple of a day. To avoid the aliasing and statistically select candidates, we masked a period range with high significance level (≤ -12.5) and used the masked range for the further analyses.
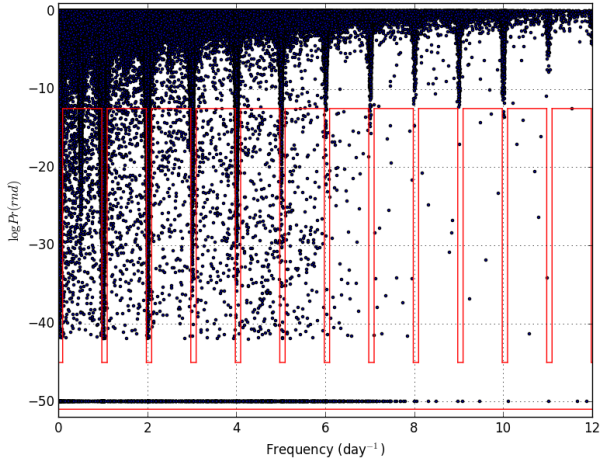

FIG. 3: $\log Pr(rnd)$ *vs frequency (day^{-1}) of $315,992$ stars selected by the quartile criteria. The region enclosed by the red lines define the masked regions with high significance level (*$\log Pr(rnd) < -12.5$*) and no aliasing (*$0.02 < frequency < 0.98$, $1.02 < frequency < 1.98$, *etc.). The masked region contains $5,658$ stars.*

5.   RR LYRAE SELECTION CRITERIA

To identify RR Lyrae stars, we applied three criteria: gri period consistency, Fourier Sine Series χ^2/ndf, and Fourier Sine Series amplitude.

5.1.   gri Period Consistency

The first criterion was the consistency of periods calculated by FLS from g, r, and i filters individually since RR Lyrae stars should have identically the same period in each filter in the range of 0.05 to 1.2 days [?] . We checked whether each filter period agreed within 0.04 days $\simeq 1$ hour with each other.

5.2.   Fourier Sine Series χ^2/ndf

The second criterion was χ^2/ndf calculated using the Fourier Sine Series (FSS). Since the RR Lyrae light curves are more or less sinusoidal, FSS with a few terms should be able to represent the light curves for certain accuracy. We used FSS in the form;

$$\text{FSS} = \sum_{n=1}^{N} \sin\left(\frac{n\pi t}{P} + \phi_n\right) \quad (1)$$

where P is the calculated period from FLS, ϕ_n is the phase, and N of up to 6 (for larger N, the computations were unstable; huge errors in the parameter estimations). We required the χ^2/ndf be within sigma deviation of 3, so χ^2/ndf $\sim \sigma^2 < 9$.

5.3.   Fourier Sine Series amplitude

The third criterion was the amplitude of FSS. As mentioned before, the amplitude range of RR Lyrae stars is 0.3 to 2.0 mags, so we set the amplitude ranges of FSS to be 0.15 to 2.15 mags by taking 10% photometry into account (1.5σ limit). The four

major types of RR Lyrae found by using out criteria are show in FIG. 4. The three criteria yielded $1,239$ RR Lyrae stars out of $5,658$ candidates in the masked region.

5.4. Period Error Estimation

Assuming the Gaussian statistics and Taylor expanding χ^2 with respect to angular frequency, the estimated error model for angular frequency, $\delta\omega$, was constructed[?] and expressed as;

$$1 = \frac{\chi^2(\omega)}{\text{ndf}} - \frac{\chi^2(\omega_0)}{\text{ndf}} \simeq \frac{A^2}{2}\delta\omega^2 \sum_{i=1}^{\text{ndp}} \frac{(t_i - \bar{t})^2}{\delta m_i^2} \quad (2)$$

where ω_0 is the calculated angular frequency by FLS, A is the calculated amplitude by FSS, ndp is the number of data points, $\bar{t}$ is our mean observation Julian Date, and δm is the uncertainty in magnitude. The choice of time origin was tricky since the model allows arbitrary time origin, so we used $\bar{t}$ as a reasonable choice. Then the period uncertainties were estimated as;

$$\delta P = \frac{d}{d\omega}\left(\frac{2\pi}{\omega}\right) = \frac{2\pi}{\omega^2}\delta\omega \,. \quad (3)$$

6. DISTANCE CALCULATIONS

In order to calculate distances to RR Lyrae stars, we needed to classify RR Lyrae subtypes as shown in FIG. 4. However, there is currently only few systematic studies (calibrations) of the type classification using light curves only (mainly on types ab and c), and they are complicated in general. To avoid the complications for the moment, we used the typical absolute RR Lyrae magnitude[?], $M_r \simeq M_v = 0.6$. To estimate the amount of dust reddening, we used the total to selective extinction[?], $Rv = 3.1$, and the number fraction weighted average color term[?], $(B - V)_0 = 0.358$, of RRab and RRc stars. The number fraction weighted average $(B - V)_0$ was calculated by using the number statistics of known RR Lyrae stars ($\simeq 91\%$ of RR Lyares are type ab and $\simeq 9\%$ of RR Lyraes are type c assuming that the numbers of Blazhko modulated and period doubling are negligible) as follows;

$$(B - V)_0 = 0.91(B - V)_{ab0} + 0.09(B - V)_{c0} \quad (4)$$

where $(B - V)_{ab0} \simeq 0.372$ and $(B - V)_{c0} \simeq 0.211$. Then the color extinction was calculated as[?];

$$E(B - V) = (B - V)_{observed} - (B - V)_0 \,, \quad (5)$$

and the extinction was calculated as[?];

$$A_v = R_v E(B - V) \quad (6)$$

Finally, the distance was calculated by using the distance modulus;

$$d = 10^{[1+(m_r - A_v - M_v)/5]} \,. \quad (7)$$

To convert the gri magnitudes to the Johnson magnitudes, the conversions given by the Sloan Digital Sky Survey (SDSS)[?] were used.

7. RESULTS

- compare with PS[?]

- density/distribution of variables in sky

- (what LS gave us for our catalog)

- put a table with 5 stars, to show off part of catalog

7.1. Spatial Distributions

From the calculated distances, the distance histogram of RR Lyrae stars is plotted and shown in FIG. 5. It almost follows the Gaussian distribution. The spatial distributions and histograms of RR Lyrae stars are shown in FIG. 6 and 7, respectively. As in FIG. 6,
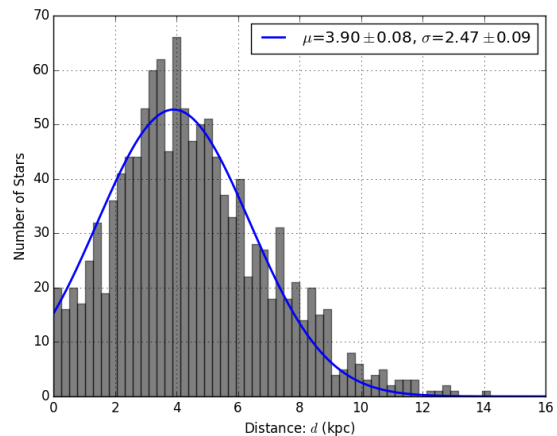

FIG. 5: *Distance histograms of 1,239 RR Lyrae stars with a Gaussian fit. The Gaussian fit was used to aid for seeing the general radial distribution of RR Lyrae stars.*
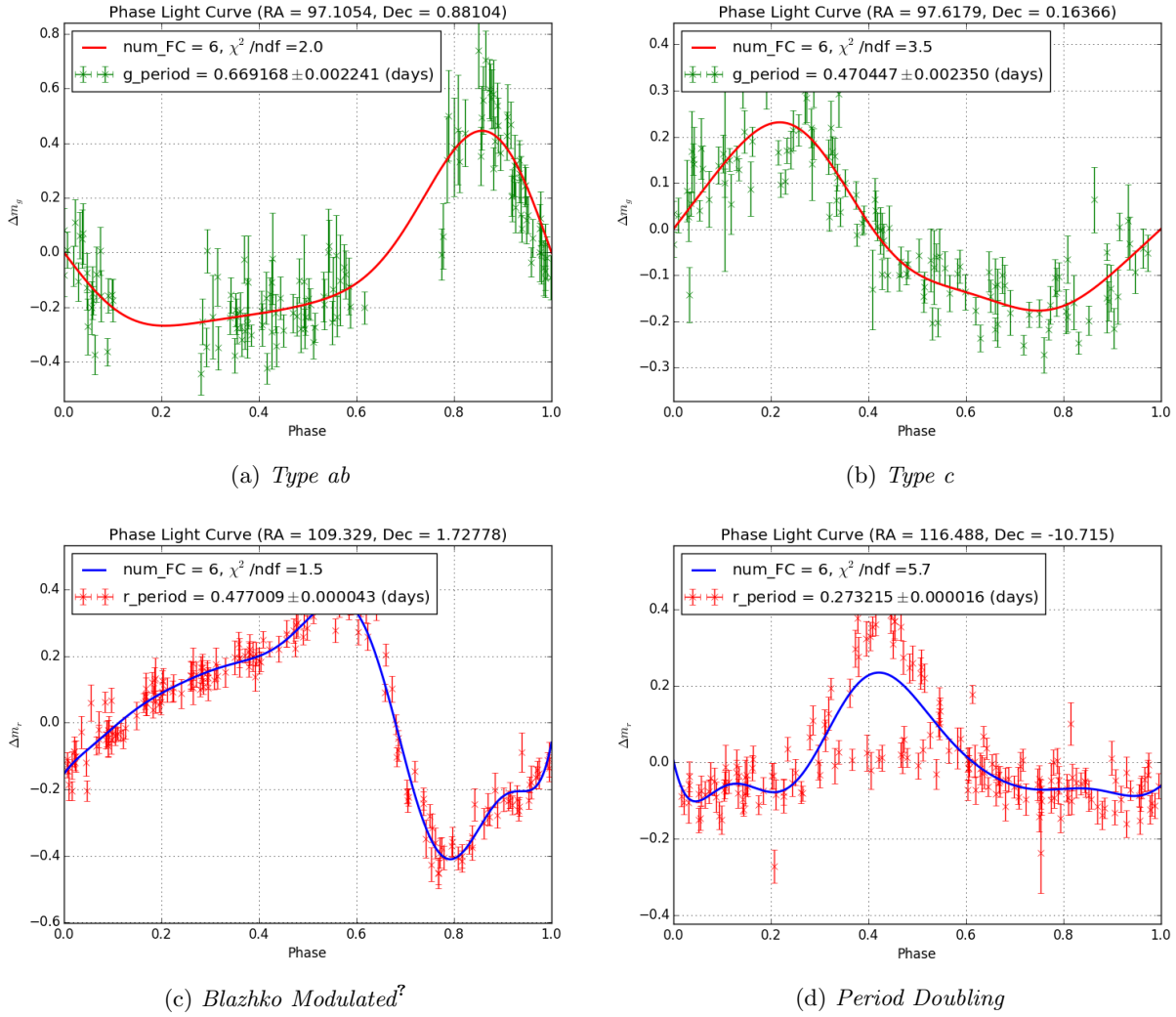
(a) *Type ab*

(b) *Type c*

(c) *Blazhko Modulated[?]*

(d) *Period Doubling*

FIG. 4: *Four major types of RR Lyrae phase light curves.*

8. EVALUATING THE HPS VARIABILITY PARAMETER

- put a table with 5 stars, to show off part of catalog

A paper, *Finding, Characterizing and Classifying Variable Sources in Multi-Epoch Sky Surveys: QSOs and RR Lyrae in PS1 3π Data*[?] (HPS), quantifies the likelihood that a star is an RR Lyrae. Using their variability statistic, $\rho_{RRLyrae}$, density and distribution of RR Lyrae and other variable candidates were determined. Table I evaluates the validity of HPS's variability criteria.

Figure 8 shows no correlation between the HPS criteria and candidates verified to be RR Lyrae stars. Of the 1.5 Billion stars identified in our FOV, we isolated the 320,000 most variable, as described in § 2 2.3.

A grouping and matching algorithm, written by

J. Tonry[?] , made it possible to isolate and group stars from various nights of observations. Implementation of logPr(rnd) allowed for complete confirmation of RR Lyrae candidates. Only stars with different variable classifications, those having lower amplitude variations, would have been able to go undetected. Masking out regions of high aliasing reduced the need to run a more rigorous analysis, due to the statistically improbability of these sources being variable. A total of 5,658 stars fell within the masked region, shown in Figure ??. FLS and FSS analysis identified 1,239 variable stars in our FOV. A defining characteristic of RR Lyrae is their variability periods, falling between 0.5 and 1.2 days. Using this restriction 279 stars were confirmed to be RR Lyrae. Variability classification was confirmed by visually inspecting the light curves of all 279 RR Lyrae and the remaining 960 unclassified variable stars. Following this procedure gives us 100% pu-
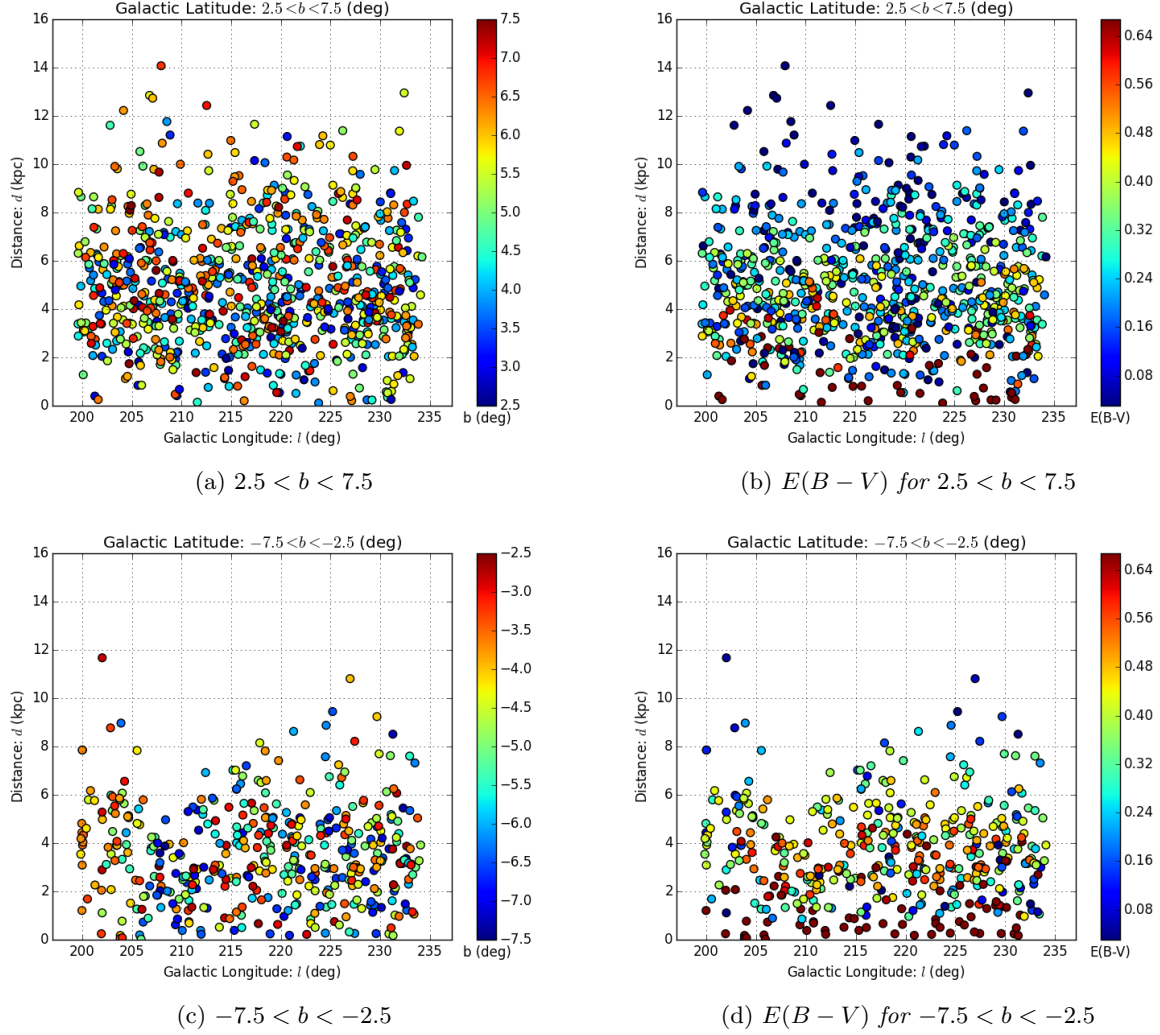
(a) $2.5 < b < 7.5$

(b) $E(B - V)$ for $2.5 < b < 7.5$

(c) $-7.5 < b < -2.5$

(d) $E(B - V)$ for $-7.5 < b < -2.5$

FIG. 6: *Spatial distributions of 1,239 RR Lyrae stars. The galactic longitude and latitude range correspond to our FOV. The range of $E(B - V)$ corresponds to the mean $E(B - V) \pm 1\sigma$.*

HPS $\rho_{RRLyrae}$	HPS_{total}	$HPS_{matched}$	RR Lyrae	Not RR Lyrae	Prob(RR)
0.0-0.05	5029	138	46	92	0.33
0.05-0.1	124	25	12	13	0.48
0.1-0.2	154	38	19	19	0.50
0.2-0.3	116	36	15	21	0.42
0.3-0.4	82	36	22	14	0.61
0.4-0.5	85	34	20	14	0.59
0.5-0.6	90	41	22	19	0.54
0.6-0.7	89	47	28	19	0.60
0.7-0.8	64	39	28	11	0.72
0.8-0.9	46	28	23	5	0.82
0.9-1.0	21	15	9	6	0.60
0.0-1.0	5900	477	244	233	0.51

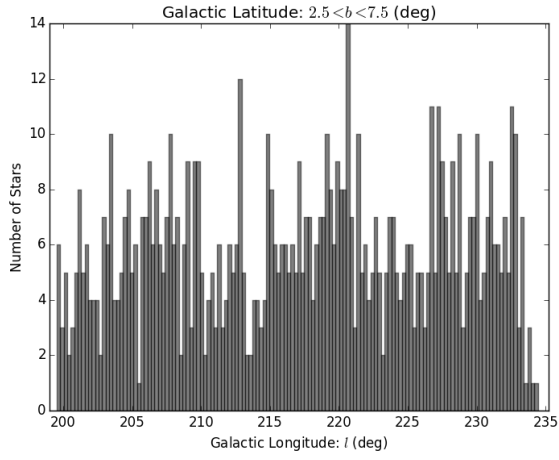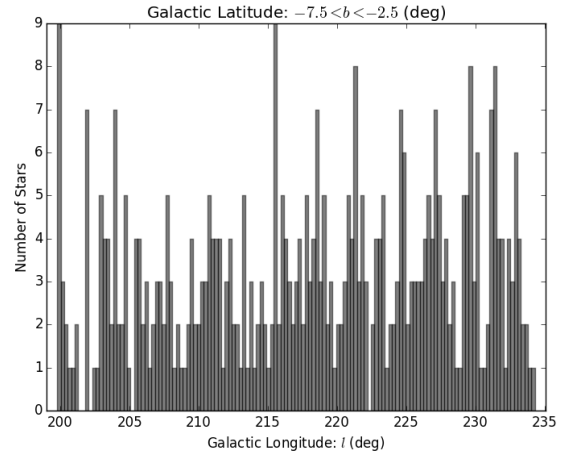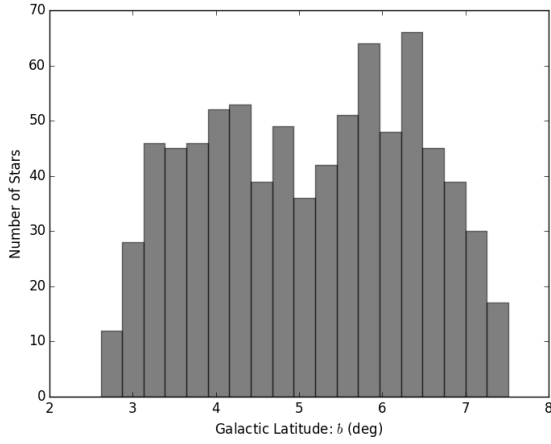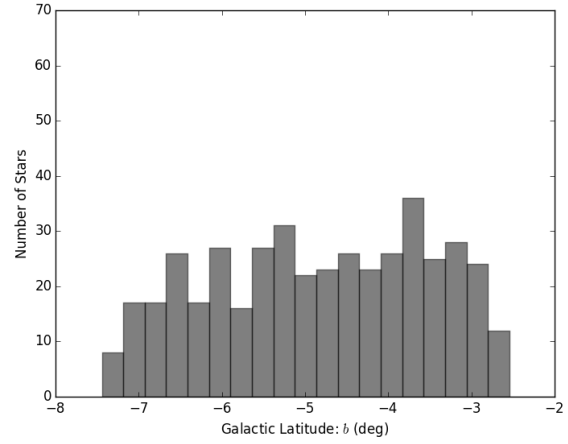TABLE I: A comparison of verified observations and HPS RR Lyrae candidates.

(a) *Galactic longitudinal histogram for* $2.5 < b < 7.5$

(b) *Galactic longitudinal histogram for* $-7.5 < b < -2.5$

(c) *Galactic latitudinal histogram for* $2.5 < b < 7.5$

(d) *Galactic latitudinal histogram for* $-7.5 < b < -2.5$

FIG. 7: *Spatial histograms of 1,239 RR Lyrae stars. The galactic longitude and latitude range correspond to our FOV.*
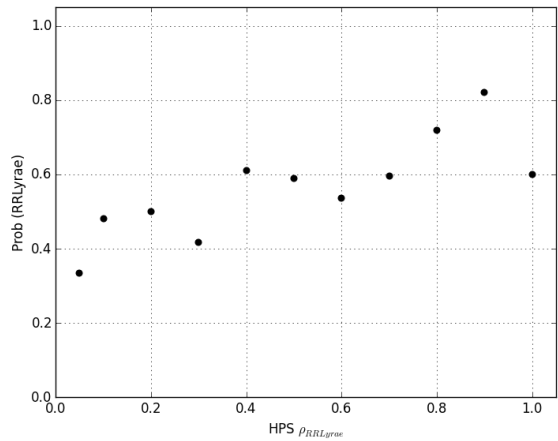
rity.

FIG. 8: *Evaluation of HPS RR Lyrae criteria.*

Using the same matching algorithm[?] made comparing observations with other variable catalogs possible. To evaluate the HPS RR Lyrae criteria, our observations were matched to stars flagged as potential RR Lyrae candidates by HPS. Shown in Table I and Figure 8, there is no correlation between HPS criteria and verified RR Lyrae stars.

9. DISCUSSION

In order to evaluate the completeness of our results, comparisons needed to be made to other variable star catalogs. Simbad[?] provided a list of variable stars within our FOV. Pulsating sources encompasses all variable objects. With 48 objects overlapping our FOV, shown in Figure 9, we achieved a completeness of 98%.

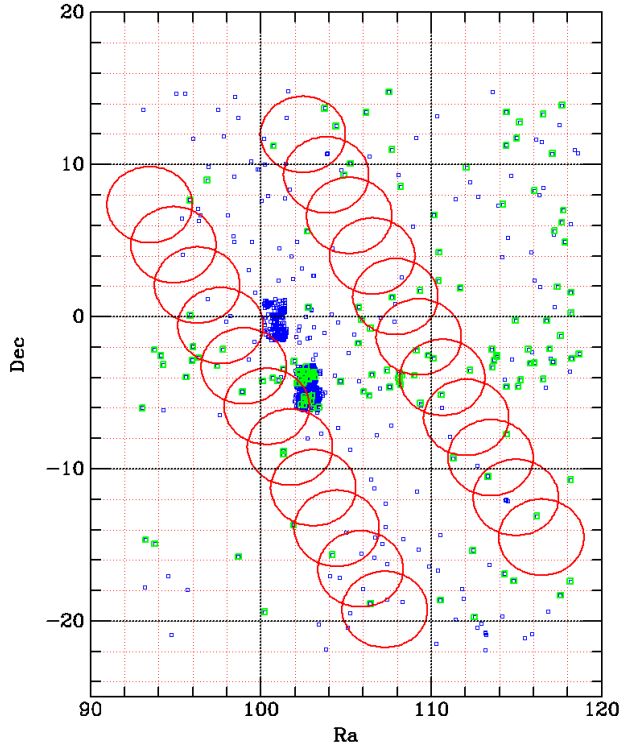[possible put two light curves in as examples of objects that overlap our field]

FIG. 9: *Observation path shown in red, with Simbad pulsators in blue and RR Lyrae in green.*

10. SUMMARY AND CONCLUSIONS

[TALK ABOUT IT]

* dhiramat@hawaii.edu
† cmutnik@hawaii.edu

A. T. impact Last Alert System, http://fallingstar.com/specifications.php (2016).

L. Molnár, R. Szabó, P. A. Moskalik, J. M. Nemec, E. Guggenberger, R. Smolec, R. Poleski, E. Plachy, K. Kolenberg, and Z. Kolláth, **452**, 4283 (2015), 1507.04714.

C. Cáceres and M. Catelan, **179**, 242-248 (2008), 0805.3704.

B. S. Rayden and B. M. Peterson, *Foundations of Astrophysics* (San Francisco: Addison-Wesley, 2010), 1st ed.

A. A. of Varaible Star Observars, https://www.aavso.org/types-variables (2012).

J. L. Tonry, personal communication (2016).

E. Magnier, in *The Advanced Maui Optical and Space Surveillance Technologies Conference* (2006), p. E50.

J. L. Tonry, C. W. Stubbs, K. R. Lykke, P. Doherty, I. S. Shivvers, W. S. Burgett, K. C. Chambers, K. W. Hodapp, N. Kaiser, R.-P. Kudritzki, et al., The Astrophysical Journal **750**, 99 (2012), URL `http://stacks.iop.org/0004-637X/750/i=2/a=99`.

W. H. Press, S. A. Teukolsky, W. T. Vetterling, and B. P. Flannery, *NUMERICAL RECIPES* (Cambridge: Cambridge University Press, 2007), 3rd ed.

J. T. VanderPlas and Ž. Ivé, **812**, 18 (2015), 1502.01344.

N. Hernitschek, E. F. Schlafly, B. Sesar, H.-W. Rix, D. W. Hogg, Ž. Ivezić, E. K. Grebel, E. F. Bell, N. F. Martin, W. S. Burgett, et al., Astrophys. J. **817**, 73 (2016), 1511.05527.

E. L. Fitzpatrick, Publications of the Astronomical Society of the Pacific **111**, 63 (1999), URL `http://stacks.iop.org/1538-3873/111/i=755/a=63`.

J. M. Nemec, **127**, 2185 (2004).

B. W. Carroll and D. A. Ostlie, *An Introduction to Modern Astrophysics* (San Francisco: Addison-Wesley, 2007), 2nd ed.

M. Fukugita, T. Ichikawa, J. E. Gunn, M. Doi, K. Shimasaku, and D. P. Schneider, **111**, 1748 (1996).

M. Wenger, F. Ochsenbein, D. Egret, P. Dubois, F. Bonnarel, S. Borde, F. Genova, G. Jasniewicz, S. Laloë, S. Lesteven, et al., aaps **143**, 9 (2000), astro-ph/0002110.